REPRINT

EUROPTO
SERIES

Reprinted from

International Symposium

Physical Concepts and Materials for Novel Optoelectronic Device Applications II

24–27 May 1993
Trieste, Italy

SPIE
P
PROCEEDINGS
SERIES

Volume 1985

Carrier lifetimes in periodically δ-doped MQW structures

Anders G. Larsson, Björn Jonsson, Ola Sjölund, and Jeffrey G. Cody

Department of Optoelectronics, Chalmers University of Technology, S-41296 Göteborg, Sweden

Thorvald G. Andersson, Shumin Wang, and Ulf Södervall

Department of Physics, Chalmers University of Technology, S-41296 Göteborg, Sweden

Daniel H. Rich

Department of Materials Science and Engineering, University of Southern California, Los Angeles, CA 90089, USA

Joseph Maserjian

Jet Propulsion Laboratory / California Institute of Technology, Pasadena, CA 91109, USA

ABSTRACT

The excitation dependent carrier recombination lifetime in periodically δ-doped strained InGaAs/GaAs multiple quantum well structures has been investigated both experimentally and theoretically. Experimentally, we find more than six orders of magnitude increase in the lifetime over that for undoped material due to the spatial separation of photogenerated carriers. This results in strong photo-optic effects and optical nonlinearities. Calculations, on the other hand, predict intrinsic recombination lifetimes in the periodically δ-doped material far above those found experimentally. Using secondary ion mass spectroscopy, transmission electron microscopy, cathodoluminescence imaging, and electron beam induced absorption modulation imaging we find evidence for misfit dislocation related recombination mechanisms that limit the carrier lifetime in the strained quantum well material.

1. INTRODUCTION

Artificially structured semiconductors are attractive for a wide variety of applications in optical signal processing[1]. For all-optical systems, where photo-optic effects and optical nonlinearities are of major interest, an increased sensitivity to the optical signal can be achieved through the use of periodic doping (alternating n and p-type)[2]. The resulting periodic variation of the conduction and valence band potentials cause a spatial separation of photogenerated carriers and consequently a reduced recombination rate. Therefore, for a given excitation intensity a larger steady state density of excess carriers can be established. The excess carriers cause a change in the optical absorption and refractive index near the bandgap[3]. By combining quantum wells and periodic doping, further improvements can be achieved through band-filling and exciton quenching effects[4] or optically induced excitonic electroabsorption[5]. In particular, the use of periodic δ-doping has resulted in very strong photo-optic effects in short period structures[6,7] through a reduction in the statistical spread of the dopants[8]. Such material has been successfully used to fabricate a low power optically addressed reflection modulator operating with normal incidence[9].

Common to all periodically doped materials is the enhancement of the carrier lifetime that determines the performance in terms of sensitivity and speed. Therefore, the carrier lifetime is a parameter of utmost importance. The onset of the photo-optic effects is limited by the spatial separation time of the photogenerated carriers and can be quite fast (on a ps-scale). The recovery, on the other hand, is determined by the enhanced carrier lifetime, and can be as long as several seconds[2].

0-8194-1234-1/93/$6.00

In this paper we present results from a comprehensive theoretical and experimental investigation of the carrier recombination in a periodically δ-doped InGaAs/GaAs multiple quantum well (MQW) structure. The InGaAs/GaAs MQW system is of particular interest, owing largely to the transparency of the GaAs substrate with respect to the MQW interband transition energies. The excess carrier lifetime and its excitation dependence is measured using a pump-probe technique. The fundamental limitations on the carrier lifetime is determined by calculating the recombination rates taking all intrinsic recombination processes into account. The material quality is accessed through secondary ion mass spectroscopy (SIMS), transmission electron microscopy (TEM) and cathodoluminescence (CL) imaging. Electron beam induced absorption (EBIA) modulation imaging is used to probe the lateral ambipolar diffusion of spatially separated carriers.

2. PERIODICALLY δ-DOPED MQW STRUCTURE

The structure under consideration is schematically shown in Fig.1. A detailed report from an experimental investigation of the photo-optic properties as well as its use for optically addressed reflection modulation has been presented previously[6,9].

The structure, which was grown by molecular beam epitaxy (MBE), consists of 44 $In_{0.2}Ga_{0.8}As$ quantum wells (QW), each 65 Å wide, separated by 780 Å thick GaAs barriers. In the center of each GaAs barrier a Be-doping plane (p-type) with a sheet density of $9.0 \cdot 10^{12}$ cm^{-2} was inserted. On both sides of the QWs, using 100 Å thick spacer layers, Si-doping planes (n-type) with a sheet density of $3.0 \cdot 10^{12}$ cm^{-2} were inserted. Ideally, these doping levels give an excess hole concentration and a space charge induced modulation depth of the conduction and valence band potentials close to the effective bandgap of the InGaAs QWs. The excess hole concentration locates the Fermi-level sufficiently far below the electron ground state in the QWs to ensure that the QWs are essentially free from electrons under thermal equilibrium. The growth temperature was 500°C to minimize redistribution of dopants during growth.

Optical excitation below the GaAs bandgap but above the fundamental bandgap of the QWs creates a uniform density of electron-hole-pairs in the QWs. The photogenerated electrons rapidly thermalize in the QWs while the holes escape into the p-δ-doped GaAs layers through thermal excitation (Fig.1). This spatial separation of the carriers reduces the recombination rate and large densities of electrons can be established in the QWs using low excitation intensities. The excess concentration of electrons modifies the QW absorption through band-filling and exciton quenching.This is shown in Fig.2a. The corresponding large change in the QW refractive index, calculated using the Kramers-Krönig relation, is shown in Fig.2b. The maximum refractive index change is 0.07.

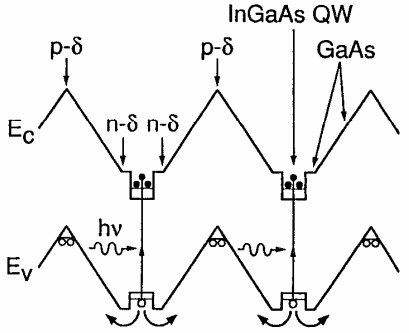

Fig.1. Energy band diagram for the periodically δ-doped InGaAs/GaAs MQW sample showing the spatial separation of photogenerated carriers.

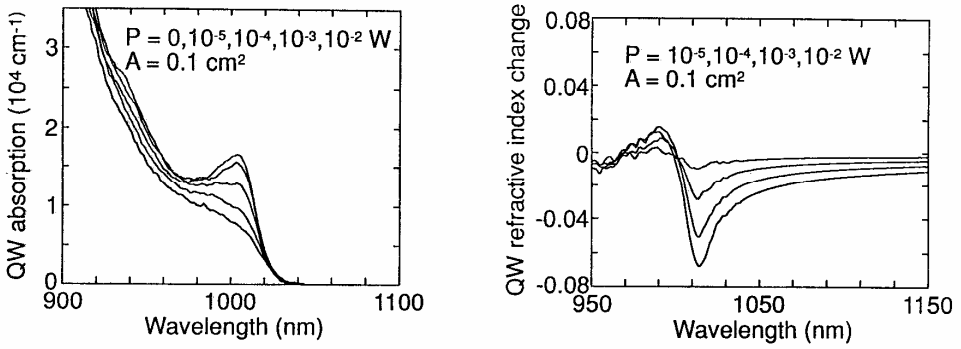

Fig.2. (a) QW optical absorption spectra recorded with various excitation intensities and (b) the associated QW refractive index change calculated from the measured absorption change.

The reduced recombination rate for spatially indirect (i.e. tunneling) transitions, as compared to spatially direct, can be understood based on the reduced overlap between the wavefunctions of the spatially separated electrons and holes. This is illustrated in Fig.3a. With optical excitation incident on the sample, the electric field produced by the spatially separated electrons and holes reduces the built-in space charge field, thus modifying the potential profile as shown in Fig.3b. The reduced modulation depth results in shallower V-shaped potential wells in the conduction and valence band. This increases the recombination rate (decreases the carrier lifetime) due to the combined effects of an increased fractional population of the QW states in the valence band and a delocalization of the carriers which increases the overlap between spatially separated electron and hole wavefunctions. In other words, periodically doped materials are characterized by an excitation dependent carrier lifetime.

3. CARRIER LIFETIME MEASUREMENTS

The carrier recombination lifetime was determined experimentally using the setup shown in Fig.4a. A narrow band (1 nm), low power (1 μW) probe signal was generated using a broad band light source and a monochromator tuned to 1000 nm where the largest excitation induced change in the optical absorption occurs (Fig.2a). As a source for optical excitation (the pump signal) we used a pseudomorphic InGaAs/GaAs single quantum well laser operating at 940 nm. The pump signal was

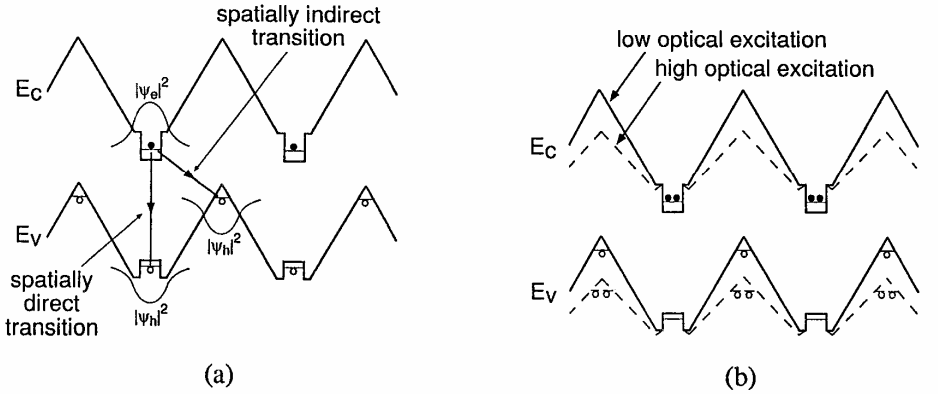

Fig.3. Energy band diagram illustrating (a) spatially direct and indirect recombination and (b) optical excitation induced modification of the potential profile.

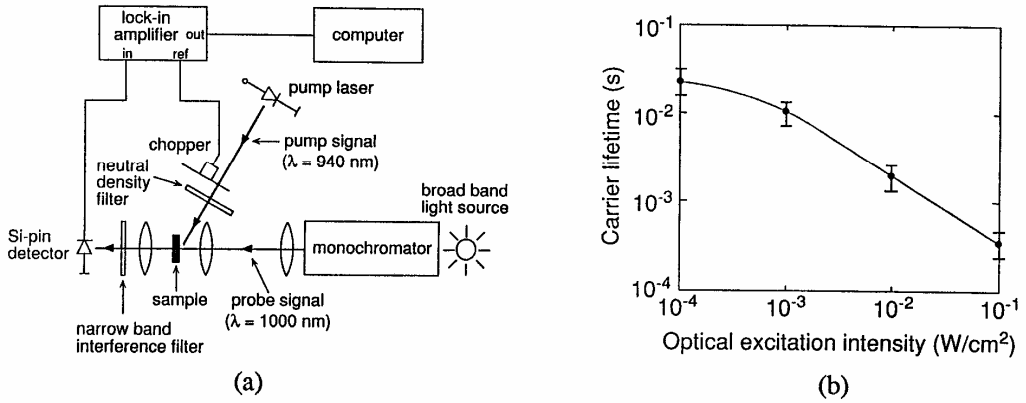

Fig.4. (a) Experimental setup for lifetime measurements and (b) measured lifetimes vs. excitation intensity.

polarized parallel to the plane of incidence and incident at Brewster angle for maximum coupling into the sample. The excitation intensity was varied using neutral density filters between the pump laser and the sample. The transmitted probe signal was recorded using a lock-in amplifier while chopping the pump signal. The frequency response of the change in the optical transmission of the probe signal induced by the pump signal, was then measured by varying the chopper frequency. Using this data we applied the technique outlined by Ando et al.[10] to deduce the carrier lifetime for various pump signal intensities. The result from this analysis is shown in Fig.4b.

From Fig.4b we conclude that the carrier recombination lifetime decreases with increasing excitation intensity. For excitation intensities in the range 10^{-3}-10^{-1} W/cm^2 the carrier lifetime varies linearly with excitation intensity. For lower excitation intensities (~ 10^{-4} W/cm^2) the carrier lifetime tends to saturate at a value of ~ 30 ms. This is most likely an apparent saturation of the lifetime since the pump signal intensity is here only a factor of ten higher than the probe signal intensity. Therefore, a non-negligible portion of the excess carrier density is generated by the probe signal itself.

4. THEORY FOR THE INTRINSIC EXCITATION DEPENDENT LIFETIME

In this section we outline the model for calculating the intrinsic carrier recombination lifetime as a function of the excess carrier density generated by optical excitation. Both spatially indirect tunneling recombination and spatially direct recombination of thermally excited carriers (Fig.3a) are considered. In order to facilitate a comparison with experimentally determined lifetimes we also calculate the spectral optical absorption in the QWs and its dependence on the excess electron density. From these spectra the steady state excess carrier density at a given excitation intensity is estimated by comparison with the measured absorption spectra (Fig.2a).

In an ideal δ-doped structure, where we neglect possible redistribution of the dopants during growth, each plane of dopants is confined to one atomic layer. This localization can conveniently be expressed by the mathematical δ-function. With a single period of the potential profile (Fig.5a) consisting of one acceptor plane at $z = z_3$ and donor planes at $z = \pm z_2$, the charge distribution Q(z) of the entire periodically doped structure under thermal equilibrium can be described by

$$Q(z) = q \cdot \sum_{i=1}^{n} [N_D \cdot \delta(z - z_2 - i \cdot z_p) + N_D \cdot \delta(z + z_2 - i \cdot z_p) - N_A \cdot \delta(z - z_3 - i \cdot z_p)] \quad (1)$$

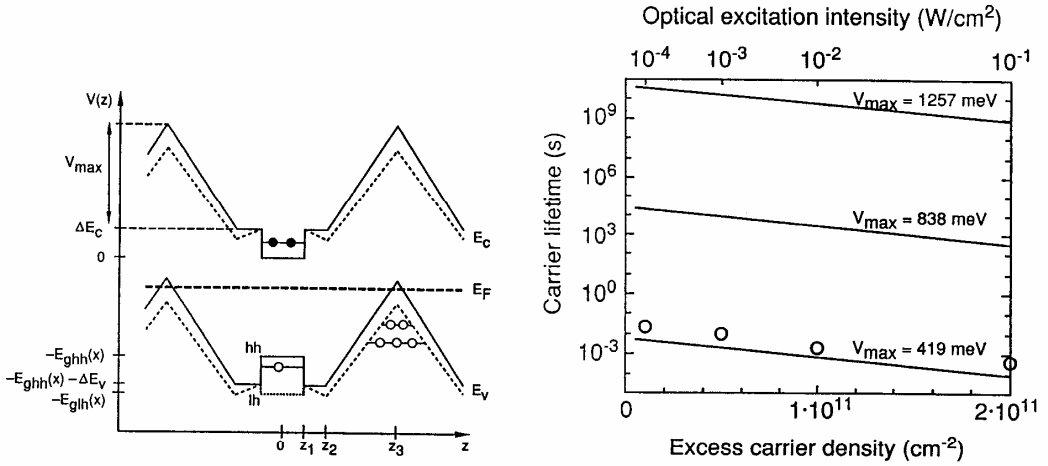

Fig.5. (a) Energy band diagram showing the coordinates and variables used to describe the potential profile. Solid line = thermal equilibrium, dashed line = optical excitation. (b) Calculated carrier lifetimes as a function of excess carrier density and the corresponding optical excitation intensity for three different amplitudes of the potential modulation. The circles indicate the measured values.

where N_A and N_D are the two-dimensional sheet densities of depleted acceptor and donor atoms, respectively. The number of periods is denoted by n and z_p is the length of one period. The resulting potential profile, V(z), may be obtained by integrating the electric field due to this charge distribution and is found to be linear as depicted in Fig.5a with an amplitude of the potential modulation, V_{max}, given by

$$V_{max} = \frac{q \cdot N_{min} \cdot d}{\varepsilon_s} \tag{2}$$

where ε_s is the dielectric constant, $d = z_3 - z_2$ is the distance from a donor plane to the nearest acceptor plane, and N_{min} is the lowest of either the donor concentration or half of the acceptor concentration

$$N_{min} = \min\left(N_D, \frac{N_A}{2}\right) \tag{3}$$

since each acceptor plane receives electrons from the two nearest neighbouring donor planes. For our particular structure the value of N_A is more than twice the value of N_D. Hence, the sheet density of donors determines the amplitude of the potential modulation and the excess free holes, located at the positions of the acceptor planes, determine the Fermi-level position under thermal equilibrium. To accurately calculate the potential profile, we have also included the effects of the biaxial compression on the strained QW potential.

Under optical excitation the potential profile is modified by the electric field produced by the photogenerated excess density, N_{ex}, of electrons in the QWs and holes (heavy and light) in the V-shaped potential wells. This electric field reduces the built-in space charge field as shown in Fig.5a. To describe this variation of the potential profile with excess carrier density we write the expressions for the potentials at z_1, z_2, and z_3 in the conduction and valence band as

$$V(z_1) = \begin{cases} \Delta E_c & ; \text{ in the conduction band} \\ -E_{ghh}(x) - \Delta E_v & ; \text{ in the valence band} \end{cases} \quad (4)$$

$$V(z_2) = V(z_1) - \frac{q}{\varepsilon_s} \cdot N_{ex} \cdot L_s \quad (5)$$

$$V(z_3) = V(z_2) + \frac{q}{\varepsilon_s} \cdot [N_{min} - N_{ex}] \cdot d \quad (6)$$

where ΔE_c is the depth of the conduction band QW, ΔE_v is the depth of the valence band QW, z_1 is half the width of the QW and $L_s = z_2 - z_1$ is the width of the spacer region on each side of the QW. This constitutes a complete description of the potential profile taking optical excitation induced modifications into account.

The electronic states in the potential profile was calculated using the transfer matrix method (TMM) which is a fast and efficient method for solving the one-dimensional time-independent Schrödinger equation in arbitrary potential profiles[12]. In the TMM, the linear potential profile is discretized into several layers where the potential and effective mass is assumed to be constant. Hence, the linear potential profile is transformed to a staircase profile. Within each layer the corresponding wavefunction can be determined. By applying appropriate boundary conditions the overall wavefunctions and energy states may be obtained numerically. Hence, by dividing the potential profile depicted in Fig.5a into 40 or 60 layers per period it is possible to find the 15–20 lowest energy states and wavefunctions with good accuracy. It should be noted that we search for quantized states not only in the QW but also in the V-shaped potential well in the valence band as well as in the region above the QW in the conduction band.

The rate of recombination between an electron state in the conduction band and a hole state in the valence band is proportional to the overlap integral between the corresponding wavefunctions[13]. Therefore, we calculate the total recombination rate, τ_{tot}^{-1}, where τ_{tot} is the associated recombination time, as an average of the recombination rates for all possible transitions, weighted by the corresponding occupation probabilities of the states involved in the transitions, according to

$$\frac{1}{\tau_{tot}} = \sum_{k=1}^{S_e} \frac{N_e(k)}{N_{tot}} \cdot \left[\sum_{m=1}^{S_{hh}} \frac{P_{hh}(m)}{P_{tot}} \cdot \frac{1}{\tau_r(k,m)} + \sum_{j=1}^{S_{lh}} \frac{P_{lh}(j)}{P_{tot}} \cdot \frac{1}{\tau_r(k,j)} \right] \quad (7)$$

where N_{tot} and P_{tot} are the total steady state free electron and hole sheet densities, respectively, established by doping and optical excitation. The reduced recombination rate between state k and m is denoted $\tau_r^{-1}(k,m)$ and the number of energy states considered in the calculations for electrons, heavy holes, and light holes are denoted S_e, S_{hh}, S_{lh}, respectively. The electron, heavy hole, and light hole sheet densities in energy state i is denoted $N_e(i)$, $P_{hh}(i)$, and $P_{lh}(i)$, respectively.

The reduced recombination rates can be calculated by multiplying the recombination rate for spatially direct transitions, $1/\tau_{dir}$, by the square of the overlap integral between the wavefunctions. Hence, the reduced recombination rate between an electron in state k in the conduction band (with wavefunction Ψ_k) and a heavy or light hole in state j in the valence band (with wavefunction Ψ_j) is given by

$$\frac{1}{\tau_r(k,j)} = \frac{1}{\tau_{dir}} \cdot I(k,j) \quad (8)$$

where $\tau_{dir} \approx 10$ ns[14] and

$$I(k,j) = \left| \int_{-\infty}^{\infty} \Psi_k(z) \cdot \Psi_j(z)\, dz \right|^2 \qquad (9)$$

is a measure of the reduction of the recombination rate as compared to spatially direct recombination. In Fig.5b we present results from the recombination lifetime calculations according to Eq.(7) as a function of excess carrier density induced by optical excitation. The results are plotted for three different sheet donor densities (N_D = $3{\cdot}10^{12}$, $2{\cdot}10^{12}$, and $1{\cdot}10^{12}$ cm^{-2}), corresponding to V_{max} = 1257, 838, and 419 meV. In order to relate the optical excitation induced excess carrier density to the excitation intensity, we have calculated the near bandgap QW optical absorption as a function of free electron density taking both band filling and exciton quenching effects into account. The details of these calculations will be presented elsewhere. Calculated absorption spectra for various electron densities are shown in Fig.6. Good agreement with measured spectra (Fig.2a) was obtained with the chosen electron densities. Therefore, we believe that these results provide a good estimation for the optical excitation induced sheet electron density for the various excitation intensities used in the lifetime measurements (Fig.5b).

Our analysis includes spatially indirect tunneling recombination as well as spatially direct transitions involving thermally populated heavy hole states in the valence band QWs. The inclusion of higher energy states was found to be crucial for the lifetime calculations since the enhanced overlap between the spatially separated electron and hole wavefunctions for these states compensates for the small occupation probabilities. We also found that the spatially indirect recombination is dominated by light hole transitions since the light carrier mass tends to delocalize the wavefunction which enhances the overlap as compared to heavy hole transitions. Furthermore, we conclude that the change in carrier lifetime with a change in doping level or optically induced excess carrier density is mainly determined by the change in the fraction of the total number of holes that occupy states in the valence band QWs.

As is evident from Fig.5b, the measured carrier lifetimes are considerably shorter than those calculated assuming an ideal structure with uniform donor and acceptor sheet densities of $3{\cdot}10^{12}$ cm^{-2} and $9{\cdot}10^{12}$ cm^{-2}, respectively. However, the rate of decrease in carrier lifetime with increasing optically induced excess carrier density is the same as the calculated and a good agreement between measured and calculated lifetimes can be achieved by assuming an effective sheet density of dopants roughly three times lower than the intended with a correspondingly lower amplitude of the potential

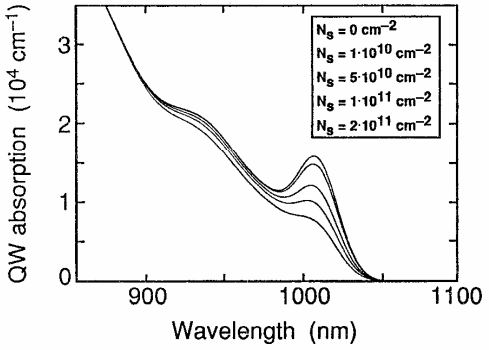

Fig.6. Calculated near bandgap optical QW absorption spectra for the periodically δ-doped InGaAs/GaAs MQW structure with various excess sheet densities of electrons as indicated.

modulation. This suggests that the carrier recombination might be governed by intrinsic mechanisms although with a smaller potential modulation than expected. One possible cause of such a reduction of the potential modulation amplitude is an extensive redistribution of the dopant atoms during growth.

5. SPATIAL LOCALIZATION OF DOPANTS

Ideally, the dopants in this δ-doped material should be localized to a single atomic layer. However, different mechanisms such as diffusion and segregation can cause a redistribution of the dopants during epitaxial growth. It has been demonstrated that under appropriate growth conditions and sufficiently low concentrations both Si and Be can be localized within a few lattice constants of GaAs[15,16]. It has also been shown that any possible internal electric fields that exist in the semiconductor during epitaxial growth can cause an electric field enhanced redistribution of the dopants[16].

The reduction of the potential modulation depth in a δ-doped doping superlattice due to dopant redistribution is illustrated in Fig.7. With ideal localization of the dopants to single atomic layers (Fig.7a), the built-in electric field E and potential modulation depth V_{max}^{2D} (Fig.7b) can be calculated by solving Poissons equation and are given by

$$E = \frac{qN_D^{2D}}{2\varepsilon_s} \tag{10}$$

$$V_{max}^{2D} = \frac{qN_D^{2D}}{2\varepsilon_s} d \tag{11}$$

where N_D^{2D} is the sheet density of donors which is assumed to be identical to the sheet density of acceptors, N_A^{2D}, ε_s is the dielectric constant of the material, d is the distance between neighbouring

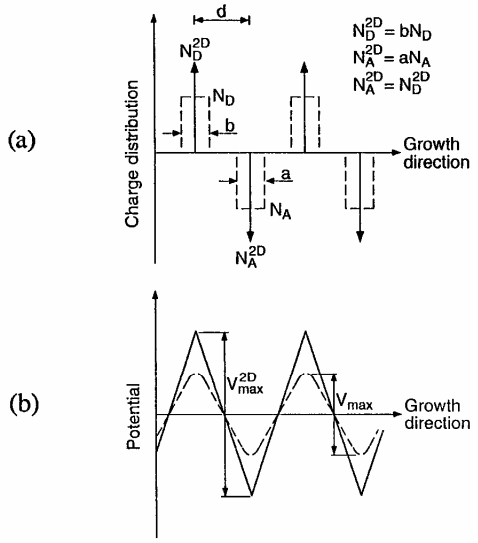

Fig.7. Illustration of the reduction of the potential modulation depth in a δ-doped doping superlattice due to dopant redistribution. (a) Charge distribution. Arrows indicate ideal planes confined to single atomic layers. Dashed lines indicate idealized rectangular dopant distributions as a result of redistribution. (b) Corresponding space charge induced modulation of the conduction and valence band potentials.

doping planes, and q denotes the elementary charge. With idealized rectangular doping profiles of width a for acceptors and b for donors after redistribution (Fig.7a) the potential modulation depth is reduced to

$$V_{max} = \frac{qN_D b}{2\varepsilon_s}\left(d - \frac{a}{4} - \frac{b}{4}\right) \qquad (12)$$

where N_D is the volumetric density of donors such that $N_D{}^{2D} = b \cdot N_D$ to maintain the same total number of donors. Similarly, $N_A{}^{2D} = a \cdot N_A$ for the acceptors. From Eq.(12) it is clear that with redistribution widths equal to the periodicity (a = b = d) the potential modulation depth is reduced by 50% as compared to the ideal case with the donors and acceptors localized to single atomic layers. Such an extensive redistribution of the dopants, possibly driven by the built-in electric field given by Eq.(10), could explain the experimentally observed carrier lifetime in the periodically δ-doped MQW structure. We have therefore investigated the spatial localization of Si and Be in periodically δ-doped GaAs.

A δ-doped GaAs sample was grown by MBE at a substrate temperature of 500 °C. The distance between neighbouring doping planes was 300 Å and they had an areal density of $3 \cdot 10^{12}$ cm^{-2}. The sample had alternating Si and Be planes with a total of 40 planes. Care was taken to reproduce the growth conditions of the periodically δ-doped InGaAs/GaAs MQW structure. Secondary ion mass spectroscopy (SIMS) was used to assess the spatial localization of the dopants in the δ-doped material using a 3.5 keV O_3^+ primary ion beam. From the obtained depth profiles of the dopant distribution we determined the full width at half maximum (FWHM) of each individual doping plane.

With this sheet density and separation between neighbouring planes the built-in electric field is 200 kV/cm according to Eq.(10). This is comparable in magnitude to the field that exists in the periodically δ-doped InGaAs/GaAs MQW sample and to that observed to cause surface segregation due to surface-induced Fermi-level pinning[16]. The electric field could therefore enhance the redistribution of the donor and acceptor ions during growth. It was also concluded by self consistent calculations that the thermally generated electron and hole densities at the growth temperature cause a negligible reduction of the internal space charge field.

The depth profiles of the impurity distributions are shown in Fig.8a for the Be and Si distributions. Fig.8b shows the Si and Be profile FWHMs as a function of depth. From comparisons with depth distributions measured for other samples with only one type of dopant where the FWHMs are limited by the resolution of the SIMS we conclude that the Si profile FWHMs are limited by the instrument resolution (40 Å). The profile FWHMs for the Be planes are, however, slightly larger than one would expect if the resolution was limited by the instrument. This could possibly be a result of an electric field enhanced redistribution of the Be ions during epitaxial growth. However, the redistribution is not large enough to cause any substantial reduction of the potential modulation in the δ-doped GaAs doping superlattice.

6. TEM AND CL IMAGING

The fact that the present sample consists of a strained InGaAs/GaAs MQW structure raises the question whether any possible structural defects generated through strain relaxation has an influence on the recombination rate. Although strain relaxation in *multiple* QW structures is not well understood we have experimentally confirmed the existence of misfit dislocations by CL and TEM measurements[17]. A CL image of the periodically δ-doped InGaAs/GaAs sample is shown in Fig.9. The wavelength used for imaging was that corresponding to the excitonic transition at the fundamental QW bandgap. Dark line defects due to misfit dislocation running along both orthogonal [100] directions are evident. Cross-sectional and plan view TEM clearly demonstrate that these misfit dislocations are confined to the MQW-to-substrate and MQW-to-cladding interfaces. The large contrast seen in the CL image, however, suggests the existence of nonradiative recombination centers

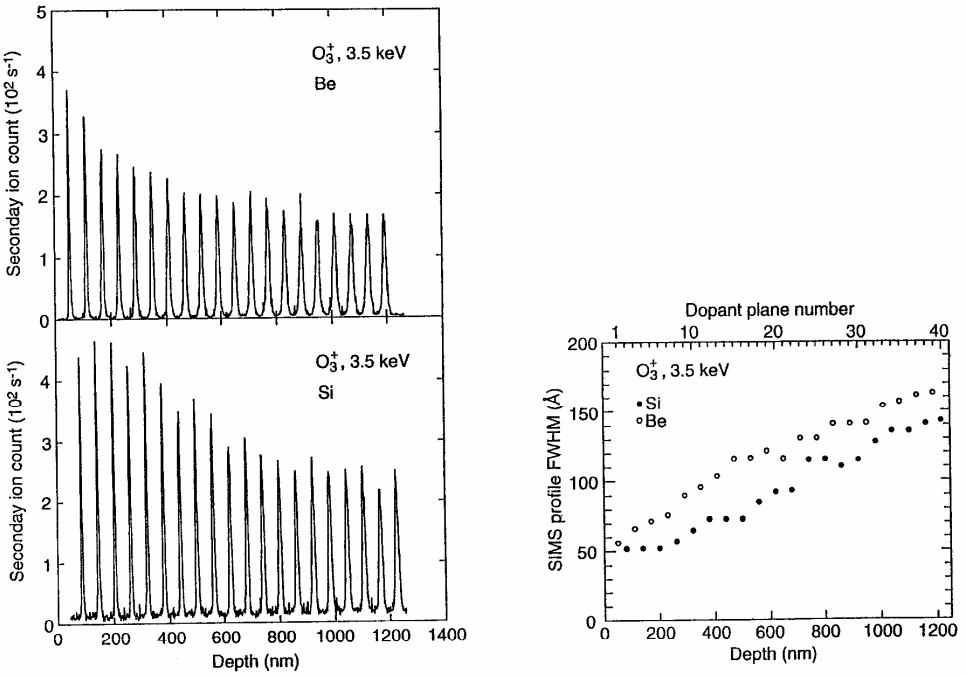

Fig.8. (a) SIMS profile of the δ-doped GaAs doping superlattice showing the Be and Si secondary ion counts. (b) Corresponding SIMS profile FWHMs of the doping planes.

spread homogeneously in the MQW material away from the dislocations. Point defects in the MQW region, left in the wake of misfit dislocation propagation and multiplication, are most likely responsible for the nonradiative recombination associated with the dark line defects[17].

7. ELECTRON BEAM INDUCED ABSORPTION MODULATION IMAGING

To study the influence of the structural defects on the carrier dynamics we have used EBIA imaging[18]. In EBIA, excess carriers are generated by a high energy electron beam within a scanning electron microscope allowing controlled excitation within a small volume. To study the absorption modulation induced by the excess carriers, a weak optical probe signal tuned to the wavelength of largest absorption change is simultaneously transmitted through the sample using optical fibers. By varying the lateral distance between the electron beam and the optical probe beam, absorption modulation images can be obtained that clearly reveal the influence of intrinsic and extrinsic recombination channels on the ambipolar diffusion of the spatially separated carriers.

Fig.10 shows intensity of CL, absorption modulation ($\Delta\alpha$), and its derivative $\partial(\Delta\alpha)/\partial x$ as a function of the distance between the optical probe signal and the electron beam obtained when moving the electron beam. The center of the steps in the absorption modulation (peaks in the derivative) are seen to correlate to the dark line defects seen in the CL image of the same area. The transport of electrons and holes is, therefore, influenced by the presence of the point defects which are spatially separated from the interface misfit dislocations. This demonstrates that extrinsic defect related mechanisms can effect the absorption modulation, excess carrier lifetime, and carrier transport.

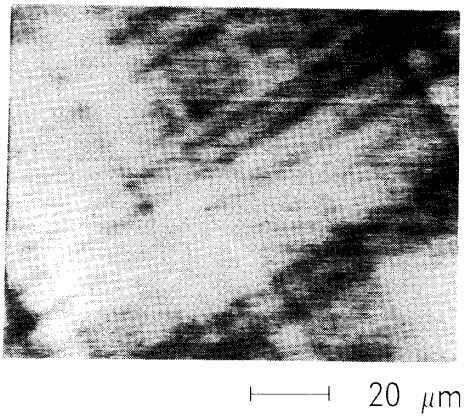

Fig.9. Scanning CL image of the exciton luminescence in the periodically δ-doped InGaAs/GaAs MQW sample.

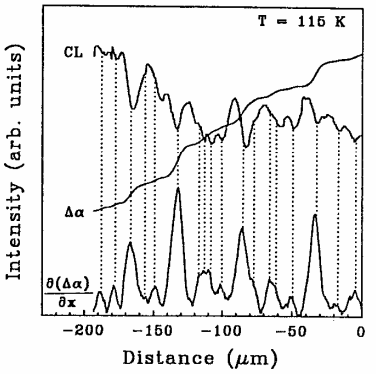

Fig.10. Histograms of CL, absorption modulation, and its derivative as a function of distance between the electron beam and the optical probe beam.

8. DISCUSSION

The results from the SIMS measurements (Fig.8) indicate a negligible redistribution of dopants under the growth conditions employed. Therefore, the amplitude of the potential modulation should be sufficiently large for the calculated intrinsic carrier lifetimes to be several orders of magnitude longer than those observed experimentally (Fig.5b). However, caution should be exercised in comparing the strained periodically δ-doped InGaAs/GaAs MQW sample with the δ-doped GaAs doping superlattice used to investigate the spatial localization of dopants.

The TEM and CL measurements show that structural defects in the form of misfit dislocations and point defects exist in the strained InGaAs/GaAs sample. The results from the EBIA measurements uniquely demonstrate that these defects influence the lateral ambipolar carrier transport. Since the diffusion coefficient for atomic diffusion is known to depend on the concentration of defects, the redistribution of dopants in the strained InGaAs/GaAs sample could therefore be enhanced with respect to the δ-doped GaAs doping superlattice if the concentration of defects is sufficiently large. As seen in the CL and EBIA images, the defect density varies laterally across the MQWs. An enhanced region of defects would then create a region of enhanced diffusion of dopants, thereby reducing the potential modulation amplitude locally with a corresponding reduction of the carrier lifetime (Fig.5b) and the ambipolar diffusion (in agreement with the EBIA images).

The strain induced defects in the MQWs could also reduce the carrier lifetime through the creation of midgap recombination centers. In addition, with increased optical excitation of the periodically δ-doped InGaAs/GaAs MQW material the attendant increase in overlap between wavefunctions of the midgap defect states and the majority carriers may cause an increase in the recombination rate similar to that for the intrinsic recombination (Fig.5b).

As a result, it seems likely that the carrier recombination lifetime is determined by misfit dislocation related recombination mechanisms.

9. CONCLUSIONS

In conclusion, we have investigated the excitation dependent carrier recombination lifetime in a periodically δ-doped InGaAs/GaAs MQW sample both experimentally and theoretically. The spatial separation of photogenerated carriers increases the carrier lifetime by more than six orders of

magnitude. Using various spectroscopic tools that probe the structural quality of the material as well as the carrier dynamics we conclude that the rate of carrier recombination is most likely governed by misfit dislocation related mechanisms in the strained material system rather than intrinsic mechanisms.

10. ACKNOWLEDGEMENTS

This work was financially supported by the Swedish Research Council for Engineering Sciences, (TFR).

11. REFERENCES

1. N. Streibl, K.-H. Brenner, A. Huang, J. Jahns, J. Jewell, A. W. Lohmann, D. A. B. Miller, M. Murdocca, M. E. Prise, and T. Sizer, "Digital optics", *Proc.of the IEEE*, Vol. 77, No. 12, pp. 1954 – 1969, Dec. 1989.
2. G. H. Döhler, "Doping superlattices ('n-i-p-i crystals')", *IEEE J. Quantum Electron.*, Vol. QE–22, No. 9, pp. 1682 – 1695, Sept. 1986.
3. A. D. Danner, P. D. Dapkus, A. Kost, and E. Garmire, "Nonlinear optical absorption in GaAs doping superlattices", *J. Appl. Phys.*, Vol. 64, No. 10, pp. 5206 – 5209, Nov. 1988.
4. J. M. Ianelli, J. Maserjian, B. R. Hancock, P. O. Andersson, and F. J. Grunthaner, "Optically controlled absorption modulator based on state filling in $In_xGa_{1-x}As/GaAs$ quantum wells", *Appl. Phys. Lett.*, Vol. 54, No. 4, pp. 301 – 303, Jan. 1989.
5. A. Kost, E. Garmire, A. Danner, and P. D. Dapkus, "Large optical nonlinearities in a GaAs/AlGaAs hetero n-i-p-i structure", *Appl. Phys. Lett.*, Vol. 52, No. 8, pp. 637 – 639, Feb. 1988.
6. A. Larsson and J. Maserjian, "Optically induced absorption modulation in a periodically δ–doped InGaAs/GaAs multiple quantum well structure", *Appl. Phys. Lett.*, Vol. 58, No. 18, pp. 1946 – 1948, May 1991.
7. A. Larsson and J. Maserjian, "Optically induced excitonic electroabsorption in a periodically δ–doped InGaAs/GaAs multiple quantum well structure", *Appl. Phys. Lett.*, Vol. 59, No. 16, pp. 1946 – 1948, Oct. 1991.
8. E. F. Schubert, "Optical properties of δ–doped doping superlattices", *Surface Science*, Vol. 228, pp. 240 – 246, 1990.
9. A. Larsson and J. Maserjian, "Optically addressed asymmetric Fabry-Perot modulator", *Appl. Phys. Lett.*, Vol. 59, No. 24, pp. 3099 – 3101, Dec. 1991.
10. H. Ando, H. Iwamura, H. Oohashi, and H. Kanbe, "Nonlinear absorption in n-i-p-i MQW structures", *IEEE J. Quantum Electron.*, Vol. 25, No. 10, pp. 2135 – 2141, Oct. 1989.
11. E. P. O'Reilly, "Valence band engineering in strained-layer structures", *Semicond. Sci. Technol.*, Vol. 4, pp. 121 – 137, 1989.
12. B. Jonsson and S. T. Eng, "Solving the Schrödinger equation in arbitrary quantum-well potential profiles using the transfer matrix method", *IEEE J. Quantum Electron.*, Vol. 26, No. 11, pp. 2025 – 2035, Nov. 1990.
13. K. Ploog and G. H. Döhler, "Compositional and doping superlattices in III–V semiconductors", *Advances in Physics*, Vol. 32, No. 3, pp. 285 – 359, 1983.
14. Y. Arakawa, H. Sakaki, M. Nishioka, and J. Yoshino, "Recombinaiton lifetime of carriers in GaAs–GaAlAs quantum wells near room temperature", *Appl. Phys. Lett.*, Vol. 46, No. 5, pp. 519 – 521, March 1985.
15. E. F. Schubert, J. B. Stark, B. Ullrich, and J. E. Cunningham, "Spatial localization of impurities in δ–doped GaAs", *Appl. Phys. Lett.*, Vol. 52, No. 18, pp. 1508 – 1510, May 1988.
16. E. F. Schubert, J. M. Kuo, R. F. Kopf, H. S. Luftman, L. C. Hopkins, and N.J. Sauer, "Be δ-doping of GaAs grown by molecular beam epitaxy", *J. Appl. Phys.* , Vol. 67, No. 4, pp. 1969 – 1979, Feb. 1990.
17. D. H. Rich, T. George, W. T. Pike, J. Maserjian, F. J. Grunthaner, and A. Larsson, "Cathodoluminescence and transmission electron microscopy study of dark line defects in thick $In_{0.2}Ga_{0.8}As/GaAs$ multiple quantum wells", *J. Appl. Phys.*, Vol. 72, No. 12, pp. 5834 – 5839, Dec. 1992.
18. D. H. Rich, K. Rammohan, Y. Tang, H.T. Lin, J. Maserjian, F. J. Grunthaner, A. Larsson, and S.I. Borenstein, "Absorption modulation induced by electron beam excitation of strained $In_{0.2}Ga_{0.8}As/GaAs$ multiple quantum wells", presented at the *20th Conference on the Physics & Chemistry of Semiconductor Interfaces*, Williamsburg, Virginia, USA, January 1993.